

Optical response of DyN

M. Azeem, B. J. Ruck, Binh Do Le, H. Warring, H. J. Trodahl et al.

Citation: *J. Appl. Phys.* **113**, 203509 (2013); doi: 10.1063/1.4807647

View online: <http://dx.doi.org/10.1063/1.4807647>

View Table of Contents: <http://jap.aip.org/resource/1/JAPIAU/v113/i20>

Published by the [American Institute of Physics](#).

Additional information on J. Appl. Phys.

Journal Homepage: <http://jap.aip.org/>

Journal Information: http://jap.aip.org/about/about_the_journal

Top downloads: http://jap.aip.org/features/most_downloaded

Information for Authors: <http://jap.aip.org/authors>

ADVERTISEMENT



AIPAdvances

Now Indexed in
Thomson Reuters
Databases

Explore AIP's open access journal:

- Rapid publication
- Article-level metrics
- Post-publication rating and commenting

Optical response of DyN

M. Azeem,^{1,a)} B. J. Ruck,¹ Binh Do Le,¹ H. Warring,¹ H. J. Trodahl,¹ N. M. Strickland,² A. Koo,² V. Goian,³ and S. Kamba³

¹The MacDiarmid Institute for Advanced Materials and Nanotechnology, School of Chemical and Physical Sciences, Victoria University, P.O. Box 600, Wellington 6140, New Zealand

²Industrial Research Limited, Lower Hutt, P.O. Box 31310, Lower Hutt 5040, New Zealand

³Institute of Physics, Academy of Sciences of the Czech Republic, Na Slovance 2, 182 21 Prague 8, Czech Republic

(Received 7 December 2012; accepted 9 May 2013; published online 28 May 2013)

We report measurements of the optical response of polycrystalline DyN thin films. The frequency-dependent complex refractive index in the near IR-visible-near UV was determined by fitting reflection/transmission spectra. In conjunction with resistivity measurements, these identify DyN as a semiconductor with an optical energy gap of 1.2 eV. When doped with nitrogen vacancies it shows free carrier absorption and a blue-shifted gap associated with the Moss-Burstein effect. The refractive index of 2.0 ± 0.1 depends only weakly on energy. Far infrared reflectivity data show a polar phonon of frequency 280 cm^{-1} and a dielectric strength of $\Delta\epsilon = 20$. © 2013 AIP Publishing LLC. [<http://dx.doi.org/10.1063/1.4807647>]

I. INTRODUCTION

Nitride compounds of rare-earth (RE) ions have gained attention due to their interesting magnetic and electronic properties. With the exception of Ce the RE ions are in their preferred trivalent state in the nitrides, so that their magnetic characters originate from their incompletely filled $4f$ shell. They are predicted to be half metals or ferromagnetic semiconductors.^{1–5} Thus they are strong candidates for use in spintronic devices, and indeed have already been demonstrated in a spin filter⁶ and as the channel in a field-effect transistor structure.⁷ Clearly in order to advance these applications, it is important to have comparative band structure information for the entire series.

Among the rare-earth nitride (REN) family, GdN is the most thoroughly studied^{8–12} compound. The Gd^{3+} ion has a half filled $4f$ shell with spin moment¹³ of $7\mu_B$. Its nitride is now a well established ferromagnetic semiconductor⁸ with $T_C = 70 \text{ K}$, though a lower^{14,15} $T_C = 30 \text{ K}$ is also reported. It has an optical energy gap^{14–16} of 1.3 eV in its paramagnetic state and 0.90 eV in its ferromagnetic state. Most of the other RENs are known to be ferromagnetic with lower Curie temperatures; the exception¹⁷ is EuN which cannot order due to the $J = 0$ state of the $4f$ shell in Eu^{3+} .

The present work describes an experimental study of the optical properties of DyN, with two more $4f$ electrons than the half-filled shell of GdN. It is a ferromagnetic semiconductor with a reported^{18,19} T_C ranging between 17 and 26 K. Its reported saturation magnetisation, $10 \mu_B/\text{Dy}$ is among the largest in the series.²⁵ Unlike GdN it has as yet not been investigated as regards its optical gap in recent stoichiometric films, and especially the role of the two filled minority-spin $4f$ bands needs to be clarified. LSDA + U electronic structure calculations³ predict that seven spin-majority $4f$ states occur in three deep narrow bands while

two $4f$ electrons go in minority-spin bands 5 eV below the top of the valence band. The same study shows a small indirect gap between the top of the valence band at Γ and the conduction band (CB) minimum at X and a minimum direct gap of 1.17 eV at X.

There are decades-old reports^{20,21} of absorption edges of almost all RENs, with the exception of CeN and PmN, though it is now recognised that those early materials were subject to the formation of nitrogen vacancies and decomposition as oxides in air. In particular, DyN has been reported to show an onset of absorption ranging^{20–22} from 0.91 eV to 2.9 eV. Preston *et al.*¹⁸ reported a measured gap value of $\sim 1.5 \text{ eV}$ between x-ray absorption and emission spectroscopies. These widely deviating claims illustrate the sensitivity of the measured results to variations in sample properties, such as stoichiometry. There is therefore a need for careful studies of the full set of optical properties of rare-earth nitrides. Here, we report reflection/transmission measurements from DyN spanning a wide range from 0.5 eV to 5.0 eV. We extract the optical constants n and k across this energy range, revealing an optical gap of 1.2 eV and relatively low value of k at energies above the gap. In films grown with reduced nitrogen concentration, we see clear evidence for free-carrier absorption and a Moss-Burstein shift of the absorption edge of several tenths of an eV. We complement our measurements of the electronic structure with far infrared (IR) reflection measurements of the zone-center phonon frequency.

II. EXPERIMENTAL DETAILS

Thin films of DyN were prepared at ambient temperature by depositing Dy at a rate of $0.5\text{--}2 \text{ \AA s}^{-1}$ in the presence of $10^{-4}\text{--}10^{-5}$ mbar of carefully purified N_2 , as has been described in more detail previously.⁸ It is expected that, as is true for GdN, a high concentration of nitrogen-vacancy donors will be found in any but the films grown in the highest N_2 pressures. The nitrogen vacancies each bind either

^{a)}E-mail: Muhammad.Azeem@vuw.ac.nz

one or two electrons, leaving at least one electron in the conduction band.²³

Before depositing the films the chamber was evacuated to a base pressure of less than 10^{-8} mbar, with O_2 partial pressure more than two orders of magnitude lower. The residual gases were reduced further by gettering with Dy before opening the shutter to expose the substrate. Due to the propensity of the rare-earth nitride thin films to oxidise in atmosphere, these films need to be passivated with a capping layer. The choice of substrate and cap was dictated by the measurements to be made: sapphire (Al_2O_3) and MgF_2 for the near-visible range, yttria-stabilised zirconia (YSZ) and Si for the far infrared. X-ray diffraction (XRD) was performed to confirm the crystal structure, lattice constant, and orientation of the films. The composition and thickness of the films were determined by Rutherford backscattering spectrometry (RBS). RBS showed stoichiometric compositions within the limited 10% reliability possible for nitrogen concentration. Table I lists growth parameters of all DyN samples used for the optical experiments.

Magnetic measurements were performed with a Quantum Design MPMS superconducting quantum interference device. The resistances of the films were monitored both *in situ* during growth and *ex situ* as a function of temperature.

Transmission and reflection spectra were obtained for $Al_2O_3/DyN/MgF_2$ in the energy range of 0.5–2.0 eV using a Fourier transform spectrometer (BOMEM model DA8) and from 1 to 6 eV using a conventional visible-UV spectrometer. A gold film and quartz wedge were used as the comparison standard for reflectance measurements in the infra-red and visible regions, respectively. Reflectance measurements were performed for light incident on both the film and the substrate surfaces, but since the transmittance is unaffected by the direction that light traverses through the sample it was taken from one side alone. The partially reflected and transmitted rays interfere to form a complex interference pattern that can compete with the loss of transmission signalling the absorption edge. In order to extract the optical constants of the DyN layer a commercial software, TFCalc,²⁴ was used which makes use of the characteristic matrix method. The data were analysed as three layers: two films (cap and DyN) and substrate, with layer thickness constrained by RBS.

The unpolarized near-normal IR reflectance spectra were taken using a Bruker IFS 113v FTIR spectrometer in the spectral range of 30–3000 cm^{-1} with a resolution of 2 cm^{-1} . Each of the reflectance spectra was evaluated as a two-layer optical system plus the substrate.²⁷ At first, the bare substrate reflectivity was measured and carefully fitted using the generalized factorized damped harmonic oscillator model

TABLE I. Growth parameters for various DyN thin films used for optical experiments.

	N_2/Dy flux ratio	α at 0.5 eV ($10^3 cm^{-1}$)	Absorption onset (eV)	Moss-Burstein shift (eV)	DyN thickness (nm)
Film A	250	0	1.2		287
Film B	75	6.5	1.5	0.3	304
Film C	22	9.7	1.7	0.5	320

$$\epsilon^*(\omega) = \epsilon' - i\epsilon'' = \epsilon_\infty \prod_j \frac{\omega_{LOj}^2 - \omega^2 + i\omega\gamma_{LOj}}{\omega_{TOj}^2 - \omega^2 + i\omega\gamma_{TOj}}, \quad (1)$$

where ω_{LOj} and ω_{TOj} are transverse and longitudinal frequencies of the j th polar phonon, respectively; γ_{LOj} and γ_{TOj} are their damping constants; and ϵ_∞ denotes the high frequency permittivity resulting from electronic absorption processes. The complex dielectric function $\epsilon^*(\omega)$ is related to the reflectivity $R(\omega)$ of the bulk substrate by

$$R(\omega) = \left| \frac{\sqrt{\epsilon^*(\omega)} - 1}{\sqrt{\epsilon^*(\omega)} + 1} \right|^2. \quad (2)$$

The high-frequency permittivity, $\epsilon_\infty = 5.88$, of the substrate resulting from the electronic absorption processes was obtained from the frequency independent reflectivity tail above the phonon frequency. When analyzing the reflectance of the substrate together with the film, we used the bare substrate parameters and adjusted only the dielectric function of the film. For this purpose, we preferentially used a classical three-parameter damped oscillator model

$$\epsilon^*(\omega) = \epsilon_\infty + \sum_{j=1}^n \frac{\Delta\epsilon_j \omega_{TOj}^2}{\omega_{TOj}^2 - \omega^2 + i\omega\gamma_{TOj}}, \quad (3)$$

where $\Delta\epsilon_j$ is the dielectric strength of the j -th mode.

III. RESULTS AND DISCUSSIONS

Figure 1 shows the XRD scan of a typical DyN film, in this case on sapphire and with a capping layer of MgF_2 . The strongest peak comes from the sapphire substrate while the next prominent peak labelled as [111] and a rather weak [222] peak confirming the cubic structure of DyN. The films are strongly [111] textured, similar to other RE nitrides grown at ambient temperature.^{8,18} The lattice constant of the films is 0.490 nm as expected¹⁸ and the average crystallite

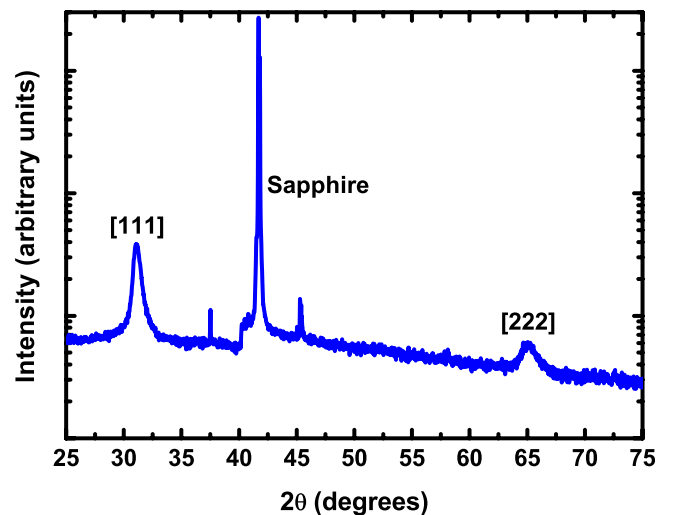


FIG. 1. XRD pattern for a representative DyN thin film. The most prominent peak comes from the sapphire substrate. Peaks labelled [111] and [222] are contributed by strongly textured DyN.

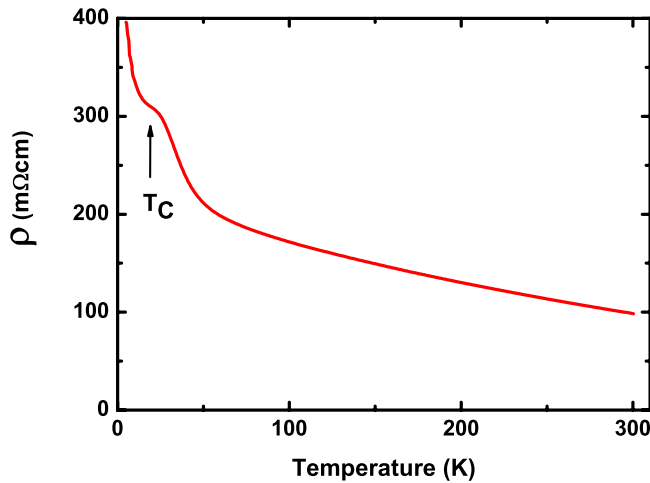


FIG. 2. Temperature dependent resistivity of a DyN thin film establishing the semiconducting nature of DyN.

size is about 10 nm as obtained using the Scherrer formula. There are no secondary phases detected in the XRD spectra.

Figure 2 shows the temperature-dependent resistivity of a film grown at high N_2 pressure. The room-temperature resistivity of $100 \text{ m}\Omega \text{ cm}$ leads then to a carrier concentration of less than 10^{20} cm^{-3} , characteristic of a moderately doped semiconductor for assumed mean free paths of 1–10 nm. Noting that each nitrogen vacancy is expected to release one electron into the conduction band, this places the vacancy concentration less than 1%. The semiconducting nature of the film is confirmed by a strongly rising resistivity with decreasing temperature. A relatively flat peak (indicated by an arrow) near the ferromagnetic Curie temperature (T_C , see below) is then followed at lower temperature by a continuation of the rise, affirming a semiconducting ground state below T_C .

The magnetic susceptibility follows the Curie-Weiss expectation with an estimated Curie temperature of 20 K (Fig. 3). However, the hysteretic behaviour of the lower-temperature ferromagnetic phase persists to higher temperature so we quote T_C as lying between 20 K and 25 K, in

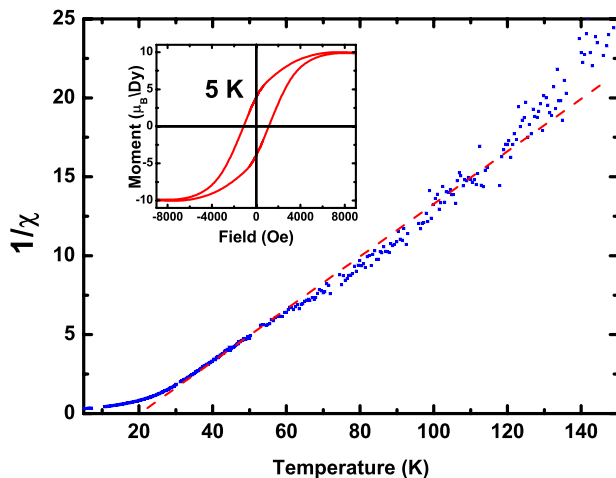


FIG. 3. Curie-Weiss plot for a DyN thin film illustrating the Curie temperature at $20 \pm 1 \text{ K}$. Inset shows hysteresis curve for DyN at 5 K in its ferromagnetic state.

agreement with the higher values found in the literature.¹⁸ Inset of Fig. 3 shows the hysteresis curve of DyN thin film at 5 K illustrating high moments of around $9.7 \pm 0.3 \mu_B/\text{Dy}$, which is close with the one found in literature.²⁵

Turning our attention towards the main features of this work, Figure 4 shows reflectance (R), transmittance (T), and their sum for Film A of the DyN sample as indicated in Table I. The film was grown under a high N_2 partial pressure. Focusing on the low energy region (0.5 eV–1.0 eV) first, we find that the absorptance ($1 - R - T$) is zero within 2% uncertainty, establishing a very low free carrier density expected of a semiconductor and signalling that this energy range is below the interband edge. Above 1.2 eV, the transmitted light falls gradually indicating the presence of interband transitions.

The interpretation of the R/T spectra was accomplished assuming the literature values for refractive indices²⁶ for the MgF_2 cap and the sapphire substrate, 1.4 and 1.8, respectively. The absorption edge of both the substrate and the cap is above the energy range for which we report the results.²⁶

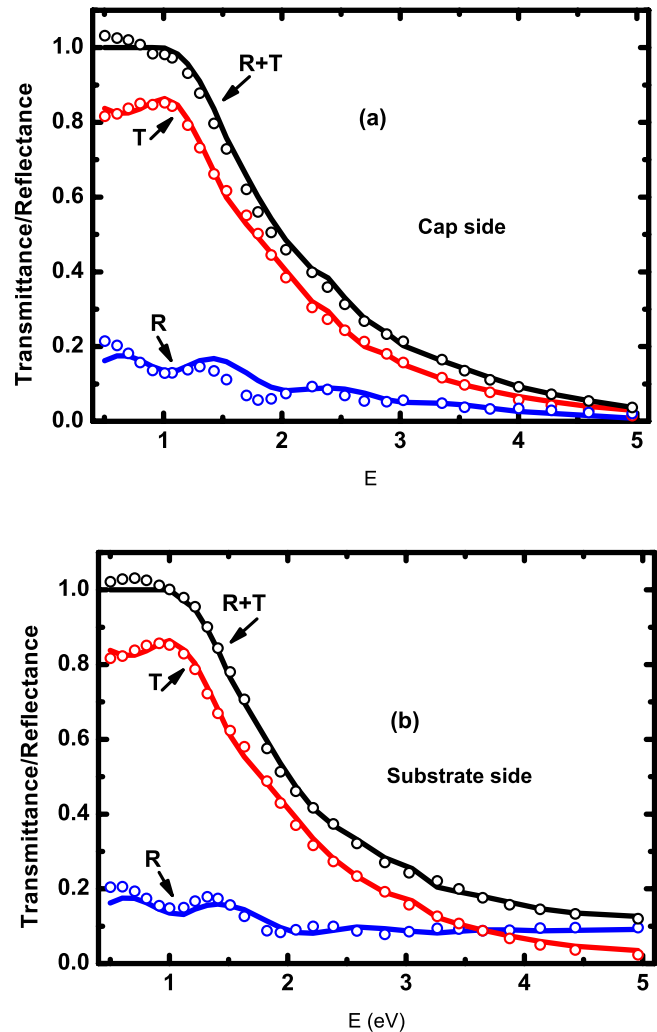


FIG. 4. (a) Reflectance from the cap side, transmittance and sum of R and T from $\approx 300 \text{ nm}$ thick DyN film (Film A) protected by a MgF_2 capping layer. Transmission drops after 1.2 eV indicating the presence of an optical gap. Open circles are experimentally obtained spectra whereas solid lines represent fitted spectra. (b) Optical spectra for the same film showing reflectance and transmittance from the substrate side.

Therefore, they do not contribute to our absorptivity measurements above the DyN gap. To first approximation, the DyN absorption below the edge was initially set to zero, as is in any case indicated by $R + T = 1$. The reflectivity in that region oscillates with the thin-film interference in the DyN and cap, but $<20\%$ average implies weak reflections at the cap/DyN and DyN/substrate interfaces. That average immediately gives a refractive index close to 2. Then fitting the reflection coefficient, including the fringes, to a full calculation gives a refractive index of 2.0 for layer thicknesses (Table I) in agreement with RBS data. Next, with this value of the refractive index approximated as constant above the edge, values of k were extracted by fitting the absorption spectra. Spectral dependence of the refractive index was then allowed, but the variations were below the level of confidence so we quote a refractive index of 2.0 ± 0.1 across the entire energy range. The circles in Figure 4 show a comparison between the calculated and the measured R/T spectra. We regard the fit as reasonable; the computer program calculates optical spectra for perfect interfaces and uniform films, but in reality one expects the films to show some degree of interface roughness.

Real and imaginary parts of dielectric function are shown in Fig. 5 for a near stoichiometric film (Film A in Table I). ϵ'' indicates that absorption increases monotonically with energy, showing no structure that might result from interband onsets at any energy above the first optical absorption edge. The rapid drop near the edge extrapolates to a gap of about 1.2 eV, with a tail to lower energy that we believe is related to uncertainties in the parameters due to incomplete correction for the interference fringes. There is only weak spectral dependence for real part, ϵ' . Turning now to a comparison with the optical parameters predicted within LSDA + U treatment, the measured gap is in excellent agreement with the predicted 1.17 eV.³ There are no published results for the absorption coefficient and the refractive index of DyN, but these measured values are in substantial disagreement with calculated results for GdN, with a very similar band structure.¹¹ That calculation resulted in a refractive index of around 3.3 and a substantially larger magnitude of

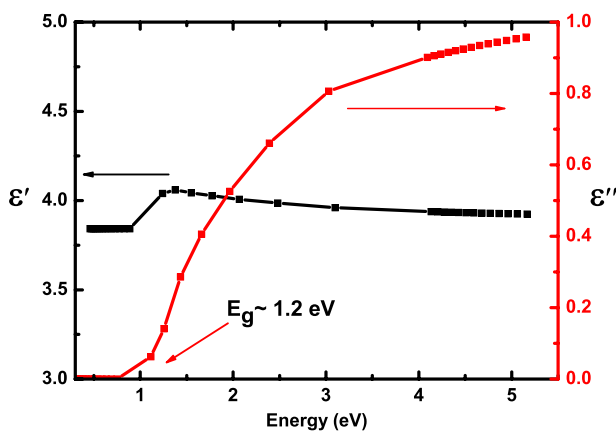


FIG. 5. Imaginary part of the dielectric function depicts the fundamental absorption edge at 1.2 eV (indicated by an arrow) for a near-stoichiometric DyN film. The real part, on the other hand, shows weak spectral dependence.

absorption coefficient than we have measured. Apparently, the dipole matrix element for the interband transitions was overestimated by the theoretical treatment.

Two further films have been studied, grown with substantially smaller excess nitrogen flux as indicated in Table I. As expected the higher density of nitrogen vacancies in these films leads to free-carrier absorption below 1.2 eV, with absorption coefficient at 0.5 eV also listed in the table. It is clear that a reduced N_2/Dy ratio leads to sub-gap absorption, as is expected for the higher density of nitrogen vacancy dopants that has earlier been reported for a lowered N_2 pressure during rare earth nitride growth.⁸ We show below that the carriers introduced by nitrogen vacancies lead not only to subgap absorption but also to a Moss-Burstein shift of the optical gap.

Figure 6 illustrates the relation between free carriers and band gap with N_2/Dy flux ratio during growth. Film A, grown with a N_2/Dy ratio of 250, is close to stoichiometric, and accordingly the subgap absorption is below the measurement limit. Films B and C, grown with lower N_2/Dy flux ratio, have a larger concentration of nitrogen vacancies and a finite sub-gap absorption. To estimate the free-carrier concentration, we note that in the high frequency limit $\omega\tau \gg 1$ the absorption coefficient is given by

$$\alpha = \frac{4\pi}{\lambda} \left(\frac{\sigma_{DC}}{2n\epsilon_0\omega^3\tau^2} \right), \quad (4)$$

where σ_{DC} is DC conductivity, λ is wavelength of the light, n is refractive index of the DyN obtained by fitting, ϵ_0 is permittivity of free space, ω is angular frequency of the light, and τ is the relaxation time of the electrons.

Applying this to the films in question, and assuming an effective mass in the conduction band of $m^* \approx 0.2m_e$ estimated from the DyN bandstructure,³ the concentration of free carriers in film A was estimated to be $<10^{20} \text{ cm}^{-3}$, in agreement with the inference drawn above from the resistivity. For films grown at lower N_2/Dy flux, we have found carrier concentrations of order 10^{21} cm^{-3} . Those carriers are accommodated in the three electron pockets at X, and then

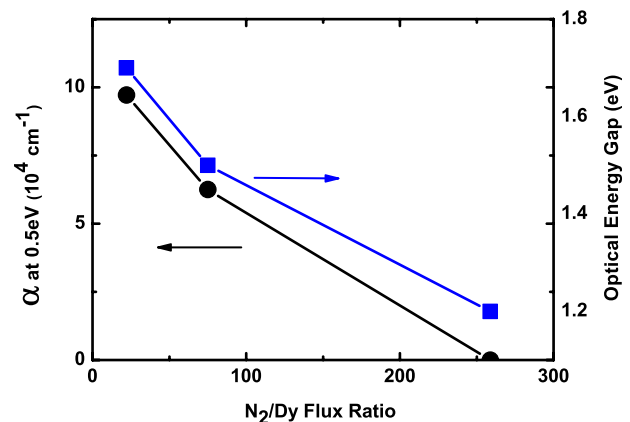


FIG. 6. Free carrier absorption (black solid circles) and the optical gap (blue solid squares) vs. N_2/Dy flux ratio during growth. Films grown with low N_2/Dy flux ratios (Films B and C from Table I) show enhanced free carrier absorption and a significant Moss-Burstein shift. Clearly, the absorption in the subgap region is correlated to the increased optical energy gap.

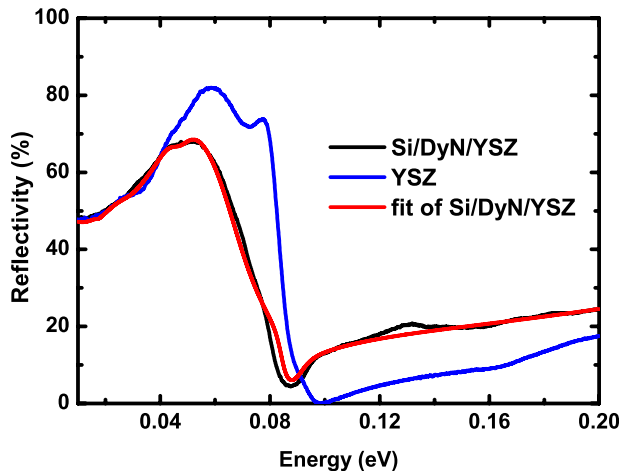


FIG. 7. Infrared reflectivity spectrum of a Y-stabilized ZrO_2 substrate, a DyN thin film on a YSZ substrate capped by amorphous Si, and the fit to the data.

introduce a degenerate electron gas of Fermi energy 0.2 eV and 0.3 eV in films B and C, respectively, in agreement with the Moss-Burstein shift of the absorption edge seen in Fig. 6. The agreement between the estimated and the observed blue-shift is excellent in light of the uncertainties in the parameters used for estimate.

Turning now to the far infrared data, we show in Figure 7 the reflectivity of the bare YSZ substrate and of the Si-capped DyN film on the YSZ substrate. These data can be fitted with only two damped oscillators; the dominant TO phonon expected in the NaCl structure is here at 280 cm^{-1} (0.035 eV), damping constant 160 cm^{-1} ; the frequency is somewhat lower than the estimated 338 cm^{-1} based on an LSDA + U approximation.⁵ The mode gives a contribution of 20 to the dc dielectric constant (Fig. 8). The satisfactory fit required also a weaker resonance at 1200 cm^{-1} , damping 2400 cm^{-1} , and dielectric contribution of 1.8. We assign this to a transition from nitrogen vacancy states expected to lie close below the conduction band.²³ The fit also returns a high-frequency dielectric constant of 4.4, in reasonable agreement with the near IR refractive index of 2.0 ± 0.1 .

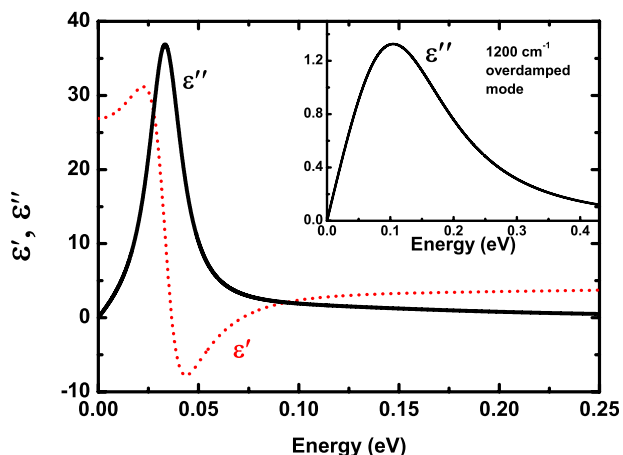


FIG. 8. Real and imaginary parts of the complex dielectric function showing the polar phonon and nitrogen-vacancy donor to conduction band transition.

IV. CONCLUSION

The optical response of DyN has been measured from 0.005 to 5.5 eV, covering both the lattice vibrational and interband regions. The direct interband gap is found at 1.2 eV in a near-stoichiometric film, with the absence of a measurable absorption below the gap establishing that DyN is a semiconductor. Films grown with sub-stoichiometric N concentration show free-carrier absorption below the gap, along with a blue-shifted absorption edge that is associated with the Moss-Burstein effect. The excess absorption and the blue shift are a result of electrons released into the CB by nitrogen vacancies. The refractive index is 2.0 ± 0.1 . Far IR results show a value of 4.4 for the high frequency dielectric function, in good agreement with the near IR refractive index. The TO phonon has a frequency of 280 cm^{-1} , close to the value predicted by an LSDA + U treatment. There is also evidence in the far IR data for a nitrogen-vacancy donor to conduction band transition at 1200 cm^{-1} .

ACKNOWLEDGMENTS

This work was supported by MacDiarmid Institute for Advanced Materials and Nanotechnology, funded by the New Zealand Centres of Excellence Fund, NZ FRST (Grant No. VICX0808), the Marsden Fund (Grant No. 08-VUW-030), and the Czech Science Foundation (Project No. P204/12/1163). Authors are grateful to John Kennedy and Peter P. Murmu for RBS measurements.

- ¹B. J. Ruck, *Nanomagnetism and Spintronics* (World Scientific, 2008), pp. 193–221.
- ²V. A. Ivanov, T. G. Aminov, V. M. Novotortsev, and V. T. Kalinnikov, *Russ. Chem. Bull.* **53**, 2357 (2004).
- ³P. Larson, W. R. L. Lambrecht, A. Chantis, and M. van Schilfhaar, *Phys. Rev. B* **75**, 045114 (2007).
- ⁴C. M. Aerts, P. Strange, M. Horne, W. M. Temmerman, Z. Szotek, and A. Svane, *Phys. Rev. B* **69**, 045115 (2004).
- ⁵S. Granville, C. Meyer, A. R. H. Preston, B. M. Ludbrook, B. J. Ruck, H. J. Trodahl, T. R. Paudel, and W. R. L. Lambrecht, *Phys. Rev. B* **79**, 054301 (2009).
- ⁶K. Senapati, M. G. Blamire, and Z. H. Barber, *Nature Mater.* **10**(11), 849–852 (2011).
- ⁷H. Warring, B. J. Ruck, H. J. Trodahl, and F. Natali, *Appl. Phys. Lett.* **102**(13), 132409 (2013).
- ⁸S. Granville, B. J. Ruck, F. Budde, A. Koo, D. J. Pringle, F. Kuchler, A. R. H. Preston, D. H. Housden, N. Lund, A. Bittar, G. V. M. Williams, and H. J. Trodahl, *Phys. Rev. B* **73**, 235335 (2006).
- ⁹F. Leuenberger, A. Parge, W. Felsch, K. Fauth, and M. Hessler, *Phys. Rev. B* **72**, 014427 (2005).
- ¹⁰K. Khazen, H. J. von Bardeleben, J. L. Cantin, A. Bittar, S. Granville, H. J. Trodahl, and B. J. Ruck, *Phys. Rev. B* **74**, 245330 (2006).
- ¹¹C. Mitra and W. R. L. Lambrecht, *Phys. Rev. B* **78**, 195203 (2008).
- ¹²A. Sharma and W. Nolting, *Phys. Rev. B* **81**, 125303 (2010).
- ¹³M. Ludbrook, I. L. Farrell, M. Kuebel, B. J. Ruck, A. R. H. Preston, H. J. Trodahl, L. Ranno, R. J. Reeves, and S. M. Durbin, *J. Appl. Phys.* **106**, 063910 (2009).
- ¹⁴H. Yoshitomi, S. Kitayama, T. Kita, O. Wada, M. Fujisawa, H. Ohta, and T. Sakurai, *Phys. Status Solidi* **8**, 488 (2011).
- ¹⁵H. Yoshitomi, S. Kitayama, T. Kita, O. Wada, M. Fujisawa, H. Ohta, and T. Sakurai, *Phys. Rev. B* **83**, 155202 (2011).
- ¹⁶H. J. Trodahl, A. R. H. Preston, J. Zhong, B. J. Ruck, N. M. Strickland, C. Mitra, and W. R. L. Lambrecht, *Phys. Rev. B* **76**, 085211 (2007).
- ¹⁷J. H. Richter, B. J. Ruck, M. Simpson, F. Natali, N. O. V. Plank, M. Azeem, H. J. Trodahl, A. R. H. Preston, B. Chen, J. McNulty, K. E. Smith,

- A. Tadich, B. Cowie, A. Svane, M. van Schilfgaarde, and W. R. L. Lambrecht, *Phys. Rev. B* **84**, 235120 (2011).
- ¹⁸A. R. H. Preston, S. Granville, D. H. Housden, B. Ludbrook, B. J. Ruck, H. J. Trodahl, A. Bittar, G. V. M. Williams, J. E. Downes, A. DeMasi, Y. Zhang, K. E. Smith, and W. R. L. Lambrecht, *Phys. Rev. B* **76**, 245120 (2007).
- ¹⁹S. Pokrant and J. A. Becker, *Eur. Phys. J. D* **16**, 165 (2001).
- ²⁰N. Sclar, *J. Appl. Phys.* **35**, 1534 (1964).
- ²¹G. Busch and P. Wachter, *Helv. Phys. Acta* **42**, 930 (1969).
- ²²J. P. Dismukes, W. M. Yim, J. J. Tietjen, and R. E. Novak, *J. Cryst. Growth* **9**, 295 (1971).
- ²³A. Punya, T. Cheiwchanchamnangij, A. Thiess and W. R. L. Lambrecht in *MRS Proceedings*, edited by W.R.L. Lambrecht, A. Ney, K. Smith, H.J. Trodahl (Mater. Res. Soc. Symp. Proc., 2011), Vol. 1290.
- ²⁴TFCalc 3.5, Software Spectra Inc., (Portland, USA, 2011).
- ²⁵O. Vogt and K. Mattenberger, "Chapter 114 Magnetic measurements on rare earth and actinide mononictides and monochalcogenides," in *Lanthanides/Actinides: Physics I*, edited by Jr. Karl A. Gschneidner, LeRoy Eyring, G.H. Lander and G.R. Choppin (Elsevier, Amsterdam, 1993), Vol. 17, pp. 301–407.
- ²⁶D. R. Lide, *Handbook of Chemistry and Physics*, 88th ed. (CRC Press, 2008).
- ²⁷V. Zelezný, I. Fedorov, and J. Petzelt, *Czech. J. Phys.* **48**, 537 (1998).